

System-size scan of dihadron azimuthal correlations in ultra-relativistic heavy ion collisions

S. Zhang^a, Y. H. Zhu^{a,b}, G. L. Ma^a, Y. G. Ma^{a*}, X. Z. Cai^a, J. H. Chen^a, C. Zhong^a

^a*Shanghai Institute of Applied Physics, Chinese Academy of Sciences, Shanghai 201800, China*

^b*Graduate School of the Chinese Academy of Sciences, Beijing 100080, China*

Abstract

System-size dependence of dihadron azimuthal correlations in ultra-relativistic heavy ion collision is simulated by a multi-phase transport model. The structure of correlation functions and yields of associated particles show clear participant path-length dependences in collision systems with a partonic phase. The splitting parameter and root-mean-square width of away-side correlation functions increase with collision system size from $^{14}\text{N}+^{14}\text{N}$ to $^{197}\text{Au}+^{197}\text{Au}$ collisions. The double-peak structure of away-side correlation functions can only be formed in sufficient “large” collision systems under partonic phase. The contrast between the results with partonic phase and with hadron gas could suggest some hints to study onset of deconfinement.

Key words: Di-hadron azimuthal correlation, Splitting parameter, Partonic transport

1. Introduction

Quantum Chromodynamics (QCD) calculation predicted an exotic quark-gluon matter in QCD phase diagram [1] may be created in the early stage of heavy ion collisions at ultra-relativistic energy [2]. For mapping the QCD phase diagram and locating QCD phase boundary and critical point [3], one needs to find a way to vary temperature (T) as well as chemical potential (μ_B). The NA61 collaboration and NA49-future collaboration [4] suggested that it can be achieved via a systematic energy (E) and system-size (A) ($E - A$) scan.

Jet quenching phenomenon has been theoretically predicted [5] and experimentally observed [6]. So far, dihadron azimuthal correlations have been demonstrated as a good method to reconstruct particle and energy distribution induced by the quenched jet. In experiment, a double-peak structure was found on the away side of dihadron azimuthal correlation functions [7, 8, 9] and the indication of conical emission of charged hadrons was reported by the STAR collaboration [10]. The centrality and transverse momentum dependences of double-peak structure of away-side correlation functions were experimentally investigated by RHIC-BNL [9, 11] and theoretically simulated in Ref. [12].

These interesting phenomena have attracted some theorists to explain the physical mechanisms for the origin of the double-peak structure. These mechanisms include a Cherenkov-like

*Corresponding author. Email address: ygma@sinap.ac.cn (Y. G. Ma)

18 gluon radiation model [13], medium-induced gluon bremsstrahlung radiation [14, 15], shock
19 wave model in hydrodynamic equations [16], waking the colored plasma and sonic Mach cones [17],
20 sonic booms and diffusion wakes in thermal gauge-string duality [18], jet deflection [19] and
21 strong parton cascade mechanism and so on [12, 20, 21, 22, 23]. Recently, Gyulassy and his col-
22 laborators suggest that the conical emission can stem from universal flow-driven mechanism [24].
23 In Ref. [25], the shock wave phenomena are discussed in viscous fluid dynamics and kinetic the-
24 ory. Renk and Neufeld [26] presented their systematic study of dependence of the Mach cone
25 signal on the energy deposition into the medium in linearized hydrodynamics. The path-length
26 effect on the correlations relative to the reaction plane are studied, respectively, by Jia et al. in
27 a simple model [27] and by Ma et al. in AMPT model [28]. In the shock wave model [16], the
28 emission angle relative to jet is calculated to be about 1.23 rad for QGP, 1.11 rad for hadronic
29 gas and zero for mixed phase. The gluon radiation mechanism for the double-peak structure [13]
30 suggests that the more energetic the jet, the smaller the emission angle. In Ref. [29], it is sug-
31 gested that the suppression or even disappearance of Mach cone at the QCD critical point due
32 to the attenuation of the sound mode. While it remains unclear what the main mechanism for
33 the emergence of the double peak structure is, all the experimental and theoretical works suggest
34 that it should depend on the nature of the hot and dense matter created in the collisions [30, 31].
35 In this paper, we study the properties of hot-dense matter produced by different system size by
36 investigating the system-size dependence of dihadron azimuthal correlations.

37 In this paper, we present participant path-length, defined as $\nu = 2N_{bin}/N_{part}$ [32] (N_{bin} and
38 N_{part} are the number of binary collision and participants, respectively), dependence of the double-
39 peak structure of away-side correlation function in the most central collisions (0-10%). The
40 structure of away-side correlation function changes near $^{40}\text{Ca} + ^{40}\text{Ca}$ collisions at $\sqrt{s_{NN}} = 200$
41 GeV in central collisions (0-10%). The results show obvious degree of freedom dependence in
42 the system with a partonic phase or with a pure hadron gas [33], which implies information of
43 the onset of deconfinement.

44 2. Model and analysis method

45 In this work, a multi-phase transport model (AMPT) [34], which is a hybrid dynamic
46 model, is employed to study dihadron azimuthal correlations. It includes four main compo-
47 nents to describe the physics in relativistic heavy ion collisions: 1) the initial conditions from
48 HIJING model [35], 2) partonic interactions modeled by a Parton Cascade model (ZPC) [36],
49 3) hadronization (discussed later), 4) hadronic rescattering simulated by A Relativistic Transport
50 (ART) model [37]. Excited strings from HIJING are melted into partons in the AMPT version
51 with string melting mechanism [38] (abbr. ‘*the Melt AMPT version*’) and a simple quark coa-
52 lescence model is used to combine the partons into hadrons. In the default version of AMPT
53 model [39] (abbr. ‘*the Default AMPT version*’), minijet partons are recombined with their parent
54 strings when they stop interactions and the resulting strings are converted to hadrons via the Lund
55 string fragmentation model [40]. The Melt AMPT version undergoes a partonic phase, while a
56 pure hadron gas is in the Default AMPT version. Details of the AMPT model can be found in a
57 review paper [34] and previous works [34, 38, 41].

58 The analysis method for dihadron azimuthal correlations is similar to that used in previ-
59 ous experiments [31, 8], which describes the azimuthal correlation between a high p_T particle
60 (trigger particle) and low p_T particles (associated particles). The raw signal can be obtained by
61 accumulating pairs of trigger and associated particles into $\Delta\phi = \phi_{assoc} - \phi_{trig}$ distributions in the
62 same event. The background which is expected mainly from elliptic flow is simulated by mixing

63 event method [31, 8]. To reconstruct the background, we accumulate pairs of one fake trigger
64 particle (high p_T) in one event and another fake associated particle (low p_T) in another event
65 to obtain the $\Delta\phi$ distribution as the corresponding background, the centralities of the above two
66 events are requested very closed. Then the background is subtracted from raw signal by using “A
67 Zero Yield At Minimum” (ZYAM) assumption as that used in experimental analysis [8] (see our
68 detailed analysis in Ref. [12]). Recently, Wang et al. [42] discussed the background in the cor-
69 relations and presented an analytical form for flow background to jet-like azimuthal correlations
70 in a cluster approach. And it is suggested that the collision geometry fluctuations and triangular
71 flow should be taken into account in the correlation analysis [43, 44, 45]. But those go beyond
72 our discussion in this paper.

73 3. Results and discussions

74 3.1. Structure of dihadron correlation function

75 The participant path-length, defined as $\nu = 2N_{bin}/N_{part}$ [32], can describe degree of multiple
76 collisions between participants in the early stage of heavy ion collisions and characterize the
77 size of the reaction zone. The n_{col}^{parton} represents average collision number of partons in the Melt
78 AMPT version. The values of ν and n_{col}^{parton} significantly increase with varying collision system
79 (CSYS) from “small” size to “large” size at $\sqrt{s_{NN}} = 200$ GeV in the most central collisions (0-
80 10%) as shown in Table 1. From this table, we can see the multiple collisions are more frequent
81 in “large” size collision system than in “small” size one. The values of N_{part} , N_{bin} and ν are
82 comparable to those from the Glauber Model [46] for both $^{64}\text{Cu} + ^{64}\text{Cu}$ and $^{197}\text{Au} + ^{197}\text{Au}$
83 collisions.

84 When the mixed background which mainly stems from elliptic flow is subtracted from the
85 raw dihadron correlation signal taken in the same events, we can get the correlation function.
86 Fig. 1 shows dihadron azimuthal correlation functions of different collision systems in the most
87 central (0-10%) collisions at $\sqrt{s_{NN}} = 200$ GeV. The correlation functions are calculated in the
88 kinetic windows, $1 < p_T^{assoc} < 3$ GeV/c as well as $2.5 < p_T^{trig} < 6$ GeV/c and $|\eta| < 1$. It shows
89 that the structure of away-side correlation function changes from the Gaussian-like distribution
90 to double-peak structure near $^{40}\text{Ca} + ^{40}\text{Ca}$ collisions with varying collision system from $^{14}\text{N} +$
91 ^{14}N to $^{197}\text{Au} + ^{197}\text{Au}$ collisions in the Melt AMPT version. In this figure, the amplitude of the
92 correlation function becomes higher with the increasing of collision system size. The associated
93 particles in the Melt AMPT version are more abundant than those in the Default AMPT version.
94

Table 1: $N_{part}(CSYS)$, $N_{bin}(CSYS)$, $\nu(CSYS) = \frac{2N_{bin}(CSYS)}{N_{part}(CSYS)}$, n_{col}^{parton} in different collision system at $\sqrt{s_{NN}} = 200$ GeV for centrality 0-10 %, the value in blanket is taken from Glauber Model [46].

CSYS	$^{14}\text{N} + ^{14}\text{N}$	$^{16}\text{O} + ^{16}\text{O}$	$^{23}\text{Na} + ^{23}\text{Na}$	$^{27}\text{Al} + ^{27}\text{Al}$	$^{40}\text{Ca} + ^{40}\text{Ca}$	$^{64}\text{Cu} + ^{64}\text{Cu}$	$^{197}\text{Au} + ^{197}\text{Au}$
$N_{part}(CSYS)$	20.78	24.25	35.92	43.61	65.97	107.04 (99.0)	343.32 (325.9)
$N_{bin}(CSYS)$	19.63	23.69	41.01	54.34	91.15	179.98 (188.8)	914.71 (939.4)
$\nu(CSYS)$	1.89	1.95	2.28	2.49	2.76	3.36 (3.8)	5.33 (5.7)
n_{col}^{parton}	1.31	1.44	1.93	2.23	2.79	3.80	7.24

95 The Default AMPT version is used to compare the properties of the double-peak structure
96 in partonic phase and in hadron gas. For investigating the properties of collision system-size

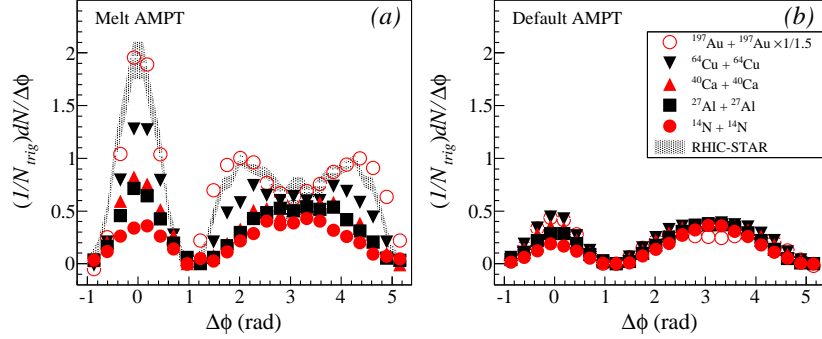


Figure 1: Dihadron azimuthal correlation functions for different collision systems in centrality 0-10% at $\sqrt{s_{NN}} = 200$ GeV; Kinetic windows: $1 < p_T^{asso} < 3$ GeV/c, $2.5 < p_T^{trig} < 6$ GeV/c, $|\eta| < 1$; the shadowing area from the STAR data [7].

97 dependences of away-side dihadron azimuthal correlations, we extract the associated particle
 98 yield N_{away}^{assoc} , splitting parameter (D) (half distance between double peaks on the away side) and
 99 Root Mean Square Width ($\Delta\phi_{rms}$) of away-side associated particles, which will be discussed in
 100 the following sections, respectively.

101 3.2. Yield of associated particles

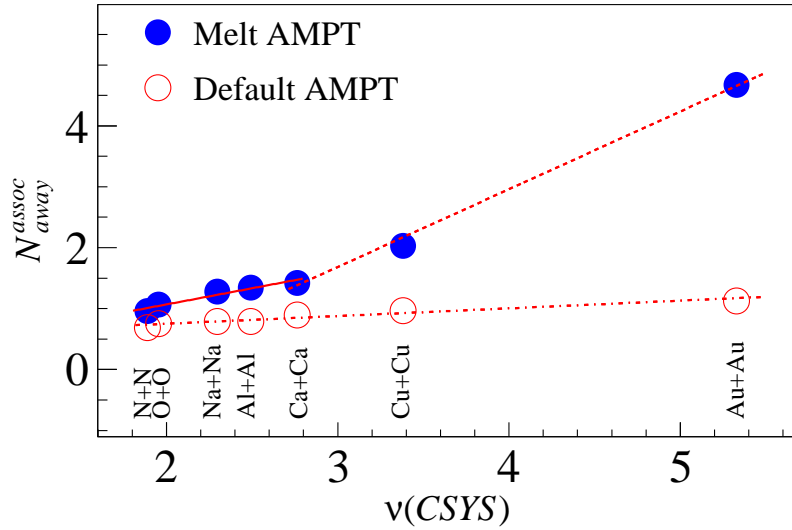


Figure 2: Yield of associated particles on away-side correlation functions, N_{away}^{assoc} , as a function of $\nu(CSYS)$ by the Melt/Default AMPT version in the centrality of 0-10% at $\sqrt{s_{NN}} = 200$ GeV.

102 The $\nu(CSYS)$ dependence of N_{away}^{assoc} is shown in Fig. 2 from the Melt/ Default AMPT version,
 103 respectively. It presents a significant increasing trend of N_{away}^{assoc} with varying the collision system
 104 from $^{14}\text{N} + ^{14}\text{N}$ to $^{197}\text{Au} + ^{197}\text{Au}$ collisions in the most central collisions (0-10%) at $\sqrt{s_{NN}} =$

105 200 GeV in the Melt AMPT version. The Default AMPT version, with a hadronic gas, does not
 106 result in a rapid increasing dependence trend. In the Melt AMPT version, the dependence trend
 107 indicates the jet correlation information can be inherited by and transmitted to more particles in
 108 a partonic phase than in a hadronic gas, especially in “large” size collision system. Furthermore
 109 it implies that the interaction strength in “large” size collision system is more significant than
 110 that in “small” size collision system, and while strong parton cascade plays a dominant role
 111 to push more away-side associated particles in the Melt AMPT version. It is interesting that
 112 the increasing slope of N_{away}^{assoc} vs $\nu(CSYS)$ from the linear fitting in the Melt AMPT version is
 113 quicker above $^{40}\text{Ca} + ^{40}\text{Ca}$ collision system, where clear double-peak structure emerges, than
 114 that in small systems. This property indicates the double-peak (Mach-like) structure can enhance
 115 associated particles yields of jet correlations partially.

116 3.3. $\Delta\phi_{rms}$ and splitting parameter on the away side

117 Root Mean Square Width ($\Delta\phi_{rms}$) of away-side correlation function is defined as

$$\Delta\phi_{rms} = \sqrt{\frac{\sum_{away} (\Delta\phi - \Delta\phi_m)^2 (1/N_{trig})(dN/d\Delta\phi)}{\sum_{away} (1/N_{trig})(dN/d\Delta\phi)}},$$

118 where $\Delta\phi_m$ is the mean $\Delta\phi$ of away-side correlation function and it approximates to π . $\Delta\phi_{rms}$
 119 can describe the diffusion degree of the associated particles relative to the direction of back jet.
 120 The $\nu(CSYS)$ dependences of $\Delta\phi_{rms}$ in the Melt/ Default AMPT version are shown in Fig. 3,
 121 respectively. $\Delta\phi_{rms}$ from the Melt AMPT version are consistent with PHENIX data [8, 47] for
 122 Cu + Cu and Au + Au collisions. $\Delta\phi_{rms}$ increases from $^{14}\text{N} + ^{14}\text{N}$ collisions to $^{197}\text{Au} + ^{197}\text{Au}$
 123 collisions in the Melt AMPT version as well as the Default AMPT version, but the increasing
 124 trend is not so quick in the later, especially for systems larger than $^{40}\text{Ca} + ^{40}\text{Ca}$. The increas-
 125 ing trend of $\Delta\phi_{rms}$ shows broadening of away-side correlation functions with increasing size of
 126 collision system. It indicates that the jet correlation information can reach faraway relative to
 127 direction of jet with changing the collision system from “small” size one to “large” size in a par-
 128 tonic phase. It is remarkable that the increasing trend of $\Delta\phi_{rms}$ from the linear fitting in the Melt
 129 AMPT version shows two different slope after and before $^{40}\text{Ca} + ^{40}\text{Ca}$ collision system, where
 130 clear double-peak structure emerges. The double peak (Mach-like) phenomenon from quenched
 131 jet can enhance the diffusion degree of the associated particles relative to back jet in the “large”
 132 size collision system. This suggests that the back jet modification in the medium created in heavy
 133 ion collisions with a partonic phase is more distinct in the “large” size collision system than in
 134 “small” size one.

135 The splitting parameter (D) is another useful observable to characterize the structure of the
 136 double-peak of away-side correlation function, and further discloses essential of jet modification.
 137 The $\nu(CSYS)$ dependence of splitting parameters (D) in the Melt/Default AMPT version are
 138 shown in Fig. 4 for the most central collisions at $\sqrt{s_{NN}} = 200$ GeV. For lighter systems from
 139 $^{14}\text{N} + ^{14}\text{N}$ to $^{27}\text{Al} + ^{27}\text{Al}$ collisions, the splitting parameter is not extracted since there is no
 140 observable double-peak structure of away-side correlation functions. In both simulation cases,
 141 the splitting parameter (D) increases from “small” size collision system to “large” size one, which
 142 indicates that there exists stronger jet-medium interaction in “large” system. It is also remarkable
 143 that the splitting parameter (D) is larger in the Melt AMPT version than that in the Default AMPT
 144 version. The Melt AMPT results are comparable to PHENIX data [9] for Cu + Cu and Au + Au
 145 collisions due to effect of parton cascade in the Melt AMPT version [12]. The parton interaction

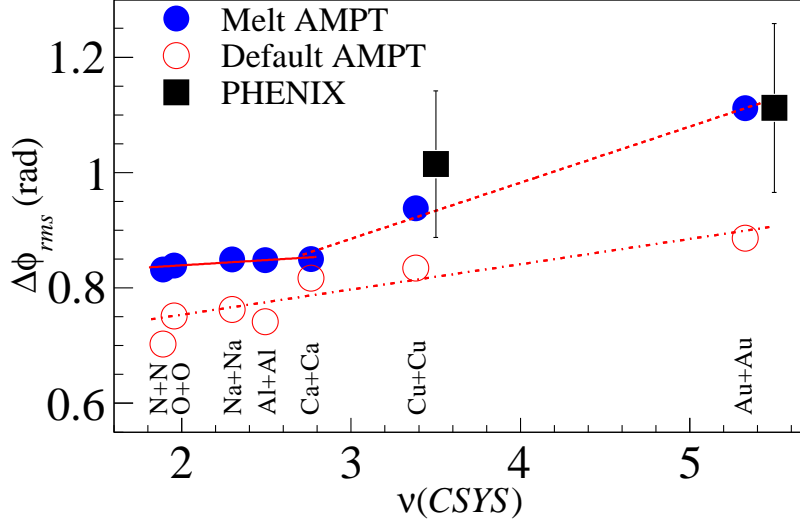


Figure 3: RMS-Width ($\Delta\phi_{rms}$) of the away-side correlation functions as a function of $\nu(CSYS)$ in the Melt/Default AMPT version for the centrality 0-10% at $\sqrt{s_{NN}} = 200$ GeV; Square from PHENIX data [8, 47].

146 cross section is taken to be 10 mb in this work, which is also reasonable for reproducing elliptic
 147 flow as well as dihadron azimuthal correlations in the Melt AMPT version [34, 38, 41, 12]. This
 148 calculation reflects that it is necessary to pass a strong partonic stage to reproduce large enough
 149 double-peak structure as the experimental data demonstrate.

150 From these results, it can be concluded that a considerable “large” collision system is neces-
 151 sary and the strong parton cascade is essential for the formation of the double-peak structure of
 152 away-side correlation function. An onset of the observable double-peak structure occurs in the
 153 mass range of $^{40}\text{Ca} + ^{40}\text{Ca}$ collision. This phenomenon indicates that the correlation is sensitive
 154 to $\nu(CSYS)$ and n_{col}^{parton} , i.e. the correlation depends on the collision system size and the violent
 155 degree of the partonic interaction in a partonic phase. Different results obtained in a partonic
 156 phase and a pure hadron gas imply the double-peak structure and jet modification are sensitive to
 157 the effective degree of freedom of the dense medium created in relativistic heavy ion collisions,
 158 which can give us some hints of the onset of deconfinement in the system-size viewpoint.

159 4. Summary

160 In summary, the present work discusses the collision system-size dependence of dihadron
 161 azimuthal correlations at $\sqrt{s_{NN}} = 200$ GeV by a multi-phase transport model. The yields of
 162 associated particles, width of away-side correlation functions and splitting parameter show sig-
 163 nificant system-size dependence. The away-side correlation function becomes more broadening
 164 with the increasing of collision system size and displays the onset of double-peak structure near
 165 $^{40}\text{Ca} + ^{40}\text{Ca}$ collisions after the system undergoes a strong partonic transport stage. These results
 166 also present the degree of freedom dependence, which might be related to onset of deconfine-
 167 ment. We would remark that these observations do not assume any dynamical mechanism for the

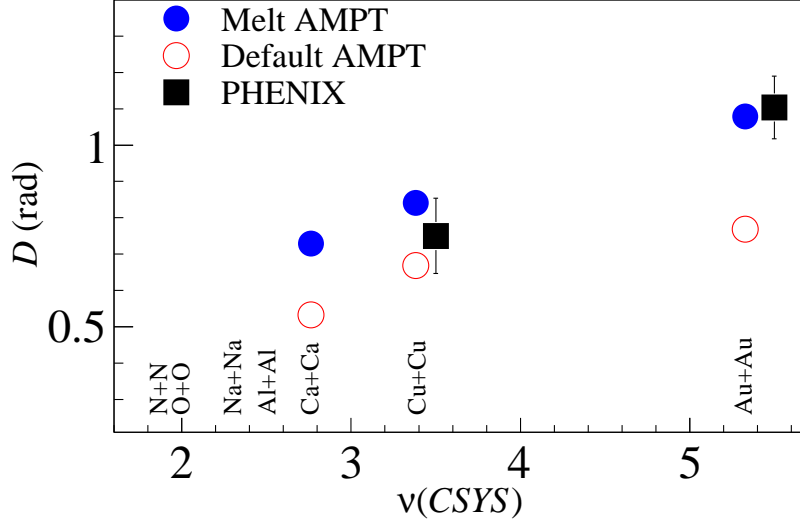


Figure 4: Splitting parameter (D) of the away-side correlation functions as a function of $\nu(\text{CSYS})$ in the Melt/Default AMPT version for the centrality 0-10% at $\sqrt{s_{NN}} = 200$ GeV; Square from PHENIX data [9].

168 formation of the double hump structure. The AMPT model would include collective Mach-like
 169 effects associated to the particles, but it would also include eccentricity fluctuating effects and
 170 triangle flow components. The result is, in this sense, robust.

171 Acknowledgements

172 This work was supported in part by the National Natural Science Foundation of China under
 173 Grant No. 11035009, 11047116, 10905085, and 10875159, 10705043 and 10705044, and the
 174 Shanghai Development Foundation for Science and Technology under contract No. 09JC1416800,
 175 and the Knowledge Innovation Project of the Chinese Academy of Sciences under Grant No.
 176 KJCX2-EW-N01, Y155017011 and O95501P0-11 and the Project-sponsored by SRF for ROCS,
 177 SEM. O819011012.

178 References

- 179 [1] F. R. Brown et al., Phys. Rev. Lett. **65**, 2491 (1990).
 180 [2] I. Arsene et al. (BRAHMS Collaboration), Nucl. Phys. A **757**, 1 (1990); B. B. Back et al. (PHOBOS Collaboration),
 181 Nucl. Phys. A **757**, 28 (2005); J. Adams et al. (STAR Collaboration), Nucl. Phys. A **757**, 102 (2005); S. S. Adcox
 182 et al. (PHENIX Collaboration), Nucl. Phys. A **757**, 184 (2005).
 183 [3] M. G. Alford et al., Rev. Mod. Phys. **80**, 1455 (2008); Frithjof Karsch, Nucl. Phys. A **698**, 199c (2002).
 184 [4] A. Laszlo et al. (NA61 Collaboration), PoS CPOD07, 054 (2007); M. Gazdzicki et al. (The NA49-future Collabo-
 185 ration), nucl-ex/0612007.
 186 [5] M. Gyulassy and M. Plümer, Phys. Lett.B **243**, 432 (1990); X. N. Wang and M. Gyulassy, Phys. Rev. Lett. **68**,
 187 1480 (1992); R. Baier, D. Schiff and B.G. Zakharov, Ann. Rev. Nucl. Part. Sci. **50**, 37 (2000).

- 188 [6] C. Adler et al. (STAR Collaboration), Phys. Rev. Lett. **91**, 072304 (2003) ; J. Adams et al. (STAR Collaboration),
189 Phys. Rev. C **73**, 064907(2006); J. Adams et al. (STAR Collaboration), J. Phys. G **34**, 799 (2007); S. S. Adler et al.
190 (PHENIX Collaboration), Phys. Rev. Lett. **91**, 072301(2003); S. S. Adler et al. (PHENIX Collaboration), Phys.
191 Rev. C **73**, 054903(2006); S. S. Adler et al. (PHENIX Collaboration), Phys. Rev. C **71**, 051902(2005).
- 192 [7] J. G. Ulery (STAR Collaboration), Nucl. Phys. A **774**, 581(2006).
- 193 [8] S. S. Adler et al. (PHENIX Collaboration), Phys. Rev. Lett. **97**, 052301(2006).
- 194 [9] Jiangyong Jia (PHENIX Collaboration),nucl-ex/0510019.
- 195 [10] B.I. Abelev et al. (STAR Collaboration), Phys. Rev. Lett. **102**, 052302 (2009); Claude A. Pruneau et al., J. Phys. G
196 **34**, S667 (2007).
- 197 [11] M. M. Aggarwal et al. (STAR Collaboration), Phys. Rev. C **82**, 024912 (2010).
- 198 [12] G. L. Ma, S. Zhang, Y. G. Ma et al., Phys. Lett. B **641**, 362(2006).
- 199 [13] V. Koch, A. Majumder, Xin-Nian Wang, Phys. Rev. Lett. **96**, 172302 (2006).
- 200 [14] I. Vitev, Phys. Lett. B **630**, 78 (2005).
- 201 [15] A. D. Polosa and C. A. Salgado, Phys. Rev. C **75**, 041901(R)(2007).
- 202 [16] J. Casalderrey-Solana et al., J. Phys. Conf. Ser. **27**, 22(2005); Nucl. Phys. A **774**, 577(2006).
- 203 [17] J. Ruppert, B. Müller, Phys. Lett. B **618**, 123(2005); R. B. Neufeld, B. Müller and J. Ruppert, Phys. Rev. C **78**,
204 041901 (2008).
- 205 [18] Steven S. Gubser, Silviu S. Pufu, Phys. Rev. Lett. **100**, 012301(2008).
- 206 [19] N. Armesto, C. A. Salgado, and U. A. Wiedemann, Phys. Rev. C **72**, 064910 (2005).
- 207 [20] G. L. Ma, Y. G. Ma, S. Zhang et al., Phys. Lett. B **647**, 122 (2007).
- 208 [21] G. L. Ma, S. Zhang, Y. G. Ma et al., nucl-th/0610088.
- 209 [22] S. Zhang, G. L. Ma, Y. G. Ma et al., Phys. Rev. C **76**, 014904 (2007).
- 210 [23] G. L. Ma, J. Phys. G **37**, 094057 (2010).
- 211 [24] B. Betz, J. Noronha, G. Torrieri, M. Gyulassy et al., Phys. Rev. Lett. **105**, 222301 (2010).
- 212 [25] I. Bouras, E. Molnár, H. Niemi, Z. Xu et al., Phys. Rev. C **82**, 024910 (2010).
- 213 [26] R. B. Neufeld and T. Renk, Phys. Rev. C **82**, 044903 (2010).
- 214 [27] J. Y. Jia, S. Esumi and R. Wei, Phys. Rev. Lett. **103**, 022301 (2009).
- 215 [28] W. Li, S. Zhang, Y. G. Ma et al., Phys. Rev. C **80**, 064913 (2009).
- 216 [29] T. Kunihiro, Y. Minami, Z. Zhang, arXiv:1009.4534.
- 217 [30] C. Adler et al. (STAR Collaboration), Phys. Rev. Lett. **90**, 082302 (2003).
- 218 [31] J. Adams et al. (STAR Collaboration), Phys. Rev. Lett. **95**,152301 (2005).
- 219 [32] W. Busza et al., Phys. Rev. Lett. **34**, 836 (1975); T. A. Trainor and Duncan J. Prindle, hep-ph/0411217; T. A.
220 Trainor, arXiv:0710.4504.
- 221 [33] S. Zhang, J. H. Chen, H. Crawford, D. Keane, Y. G. Ma, Z. B. Xu, Phys. Lett. B **684**, 224 (2010).
- 222 [34] Z. W. Lin, C. M. Ko, B. A. Li, B. Zhang, S. Pal, Phys. Rev. C **72**, 064901 (2005).
- 223 [35] X. N. Wang and M. Gyulassy, Phys. Rev. D **44**, 3501 (1991) ; M. Gyulassy and X. N. Wang, Comput. Phys.
224 Commun. **83**, 307 (1994) .
- 225 [36] B. Zhang, Comput. Phys. Commun. **109**, 193 (1998) .
- 226 [37] B. A. Li and C. M. Ko, Phys. Rev. C **52**, 2037 (1995).
- 227 [38] Z. W. Lin, C. M. Ko, Phys. Rev. C **65**, 034904 (2002); Z. W. Lin, C. M. Ko et al., Phys. Rev. Lett. **89**, 152301
228 (2002).
- 229 [39] B. Zhang, C. M. Ko et al., Phys. Rev. C **61**, 067901 (2000).
- 230 [40] B. Andersson, G. Gustafson et al., Phys. Rep. **97**, 31(1983).
- 231 [41] J. H. Chen, Y. G. Ma, G. L. Ma et al., Phys. Rev. C **74**, 064902 (2006).
- 232 [42] Q. Wang and F. Q. Wang, Phys. Rev. C **81**, 014907 (2010).
- 233 [43] B. Alver and G. Roland, Phys. Rev. C **81**, 054905 (2010).
- 234 [44] Jun Xu and Che Ming Ko, Phys. Rev. C (in press), arXiv:1011.3750
- 235 [45] G. L. Ma and X. N. Wang, arXiv:1011.5249.
- 236 [46] B. I. Abelev et al. (STAR Collaboration), Phys. Lett. B **673**, 183 (2009) .
- 237 [47] W. G. Holzmann (PHENIX Collaboration), AIP Conf. Proc. **842**, 50 (2006) .